

Adaptive Edge-Directed Interpolation Using Edge Map Analysis

DAEJUN PARK, JECHANG JEONG

Department of Electronics and Computer Engineering
Hanyang University
222 Wangsimni-ro, Seongdong-gu, Seoul 04763
Republic of Korea
daejoon12@hanyang.ac.kr, jjeong@hanyang.ac.kr

Abstract: - In this paper, an edge-directed interpolation is proposed using edge map analysis. Conventional algorithms have various disadvantages (edge blurring effect, excessive computational complexity, etc.) by performing interpolation without distinguishing between flat and edge regions. Therefore, it is possible to overcome the drawbacks and limitations of the existing algorithms by applying the optimal interpolation technique to the flat area and the edge area through edge map analysis. The comparison of objective and subjective experimental results shows that the proposed algorithm shows better performance than the existing algorithms.

Key-Words: - Image interpolation, edge-directed interpolation, bilinear interpolation, bicubic interpolation, edge map analysis, edge map prediction

1 Introduction

Pixel interpolation is an image processing technique that extends the size of a digital image [1]. It proceeds through extracting available information from a given image. Various algorithms can be developed according to the information extraction method, and the performance of the algorithm varies depending on the method of utilizing the extracted information. Therefore, it is possible to select the optimal image interpolation method according to the field of performing the image interpolation.

A method of generating a HR (High Resolution) image from a LR (Low Resolution) image can be divided into a method of considering the edge direction and a method of not considering the edge direction. Conventional algorithms that do not consider the edge direction are pixel replication, bilinear, bicubic, cubic spline interpolation, interpolation technique through frequency domain conversion and so on [2-5]. Unfortunately, these techniques are effective for interpolating low frequency regions that are responsible for the shape of an image. But image quality degradation such as blurring and stair-case artifact occurs in a high frequency region where human visual system is sensitive.

Therefore, maintaining the sharpness of the edge and eliminating the deterioration of image quality has been developed as a basic condition for improving the picture quality of the pixel interpolation technique. As a result, the algorithm

considering the edge direction has become the mainstream of the pixel interpolation technique. The most famous algorithm is NEDI (New Edge-Directed Interpolation) [6]. NEDI performs image interpolation through HR covariance prediction using geometric duality between the LR covariance and the HR covariance. However, there is a fatal disadvantage that the image quality deteriorates in a high frequency region where the edge is not obvious like a texture. And the execution time is also long.

This paper proposed an adaptive edge-directed pixel interpolation scheme based on pixel distribution by separating flat pixels and edge pixels using edge map analysis. After decomposing the low frequency and high frequency of the LR image, the Sobel operator is applied to the low frequency to construct an edge map. After determining the flat/edge distribution of the current pixel to be interpolated by grasping the flat/edge distribution of the surrounding pixels, an appropriate interpolation technique is performed. In the flat region, a bilinear interpolation method using four neighboring pixels is applied. In the edge region, an edge-directed interpolation technique is applied though directional inheritance of neighboring pixels and comparison of dispersion of reference pixels. If it is a texture area, which is hard to determine the flat/edge characteristic of the current pixel, we perform appropriate interpolation by comparing the distribution of reference pixels of all the interpolation methods in this paper.

This paper is organized as follows. In Section 2, we describes the existing algorithms. In Section 3, the proposed algorithm, adaptive edge-directed interpolation using edge map analysis, is introduced. In section 4, experimental results are presented and analyzed to demonstrate the superiority of the proposed algorithm. Finally, we conclude this paper with conclusions in Section 5.

2 Conventional Algorithms

2.1 Bilinear Interpolation

Bilinear interpolation, which is one of the most basic image interpolation algorithms, is a two-dimensional extension of linear interpolation. As shown in Fig.1, interpolation is performed using four adjacent pixels. The sum of the pixel values multiplied by the weight inversely proportional to the distance of the reference pixels is taken as the pixel value of the HR image. The weights used in this process are determined linearly and are obtained as follows.

$$\begin{aligned} E &= (1-x)A + xB \\ F &= (1-x)C + xD \\ P &= (1-y)E + yF \end{aligned} \tag{1}$$

The pixel P is a HR pixel to be interpolated, and is obtained by performing one-dimensional linear interpolation on the x-axis and the y-axis using the pixels A, B, C and D.

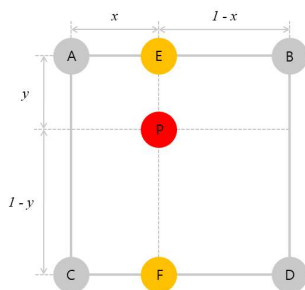


Figure 1 Bilinear Interpolation

2.2 Bicubic Interpolation

Since the bilinear interpolation introduced in Section 2.1 uses a linear weight inversely proportional to the distance, blurring artifact occurs. In order to solve this problem, a method of applying cubic convolution function to the weight is proposed. The cubic convolution function was first introduced by Rifman and improved by Keys and Bernstein. A

function for determining a weight for a pixel is as follows.

$$f(x) = \begin{cases} (a+2)|x|^3 - (a+3)|x|^2 + 1, & 0 \leq |x| < 1 \\ a|x|^3 - 5a|x|^2 + 8a|x| - 4a, & 1 \leq |x| < 2 \\ 0, & 2 \leq |x| \end{cases} \tag{2}$$

The appropriate values of ‘a’ are -0.5 for Keys, and -1 for Rifman and Bernstein [3,7,8].

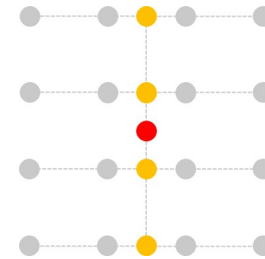


Figure 3 Bicubic Interpolation

3 Proposed Algorithm

In this paper, we propose a method to determine the flat/edge of HR pixels to interpolate through edge map analysis and to perform appropriate interpolation method for each pixel. Also, interpolation is performed by determining the optimal interpolation method for the texture region, which is difficult to determine the flat/edge characteristics. The overall flowchart of the proposed algorithm is shown in Fig.3.

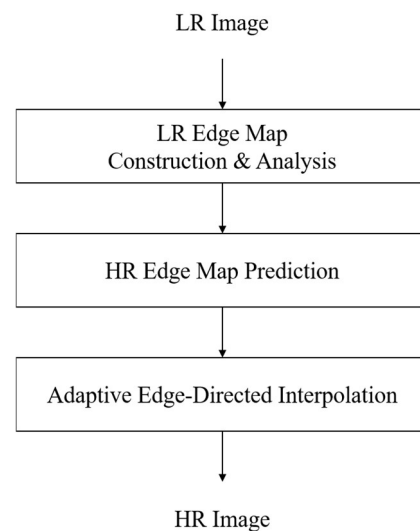


Figure 3 Flowchart of the Proposed Algorithm

3.1 LR Edge Map Construction & Analysis

A LR image, which is an input value, is separated into a low frequency and a high frequency using a low-pass filter, and an edge map is constructed by applying a Sobel operator to a low-frequency. After calculating the edge intensity and direction value for each pixel, it is classified into edge when the edge intensity of the current pixel is larger than the average edge intensity of the image. The edge direction values are classified into four directions of horizontal, vertical, 45 degree angle and 135 degree angle. The edge map construction of the LR image is performed through the above classification procedure.

A		B
	X	
C		D

	B	
A	X	D
	C	

Case	A	B	C	D	Case	A	B	C	D
1	S	S	S	S	9	E	E	S	E
2	E	E	E	E	10	E	E	E	S
3	E	S	S	S	11	E	E	S	S
4	S	E	S	S	12	E	S	E	S
5	S	S	E	S	13	S	S	E	E
6	S	S	S	E	14	S	E	S	E
7	S	E	E	E	15	E	S	S	E
8	E	S	E	E	16	S	E	E	S

Table 1 Selection of Surrounding Pixels and 16 Characteristic Distributions

The flat/edge distribution of the four pixels surrounding the pixel to be interpolated with the HR image has a total number of 16 cases as shown in Table 1. Assuming that the structural characteristics between the LR image and the HR image are similar, the ratio of the occurrence of each case and the flat/edge of the pixel to be interpolated can be predicted through analysis of the LR image edge map.



Case _i	p(Case _i)	p _{LR} (P=Smooth Case _i)	p _{LR} (P=Edge Case _i)
1	0.5349	0.9969	0.0031
2	0.2131	0.0009	0.9991
3	0.0233	0.9692	0.0308
4	0.0139	0.8632	0.1368
5	0.0144	0.8360	0.1640
6	0.0236	0.9580	0.0420
7	0.0214	0.0513	0.9487
8	0.0145	0.0937	0.9063
9	0.0143	0.0598	0.9402
10	0.0216	0.0226	0.9774
11	0.0104	0.5935	0.4065
12	0.0381	0.5204	0.4796
13	0.0120	0.5573	0.4427
14	0.0375	0.5254	0.4746
15	0.0045	0.1854	0.8146
16	0.0025	0.8571	0.1429

Table 2 Example of Probability Distribution of Interpolation Pixel Characteristics

3.2 HR Edge Map Prediction

As shown in Table 2, the HR image edge map prediction is performed using the flat/edge distribution probabilities of the four pixels surrounding the current pixel, which have a total of 16 cases obtained from the LR image edge map analysis. In each case, the pixel to be interpolated is divided into flat/edge, so there are 32 probabilities in total. As shown in Fig.4, it is assumed that the probability distribution of pixel characteristics is similar in LR image and HR image.

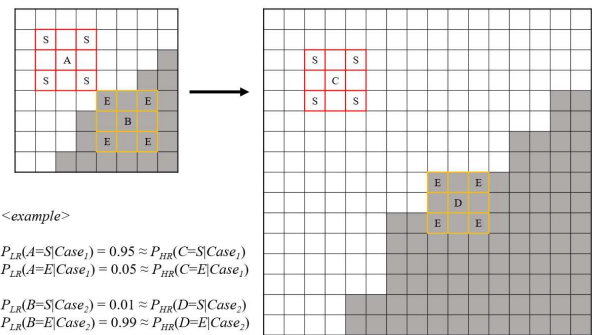


Figure 4 Example of Comparison of Structural Characteristics between LR image and HR image

First, a LR image edge map is mapped to a HR image edge map. The edge map prediction of the diagonal shape is performed first, and it is necessary to understand which distribution the four pixels in the direction of 45 degrees and 135 degrees of the pixel to be interpolated belong to. If the probability of flat or edge in the probability table exceeds the specific threshold value, the current pixel is determined as the corresponding characteristic. If the flat/edge probability is lower than the threshold value, it is classified as a texture area and used later in the image interpolation process.

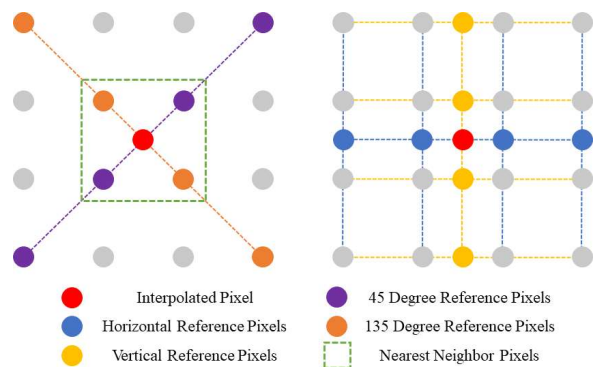


Figure 5 Diagonal Interpolation

After the diagonal edge map prediction is performed as shown in Fig.5, the cross-shaped edge map prediction is performed twice to complete the HR image edge map prediction as shown in Fig.6.

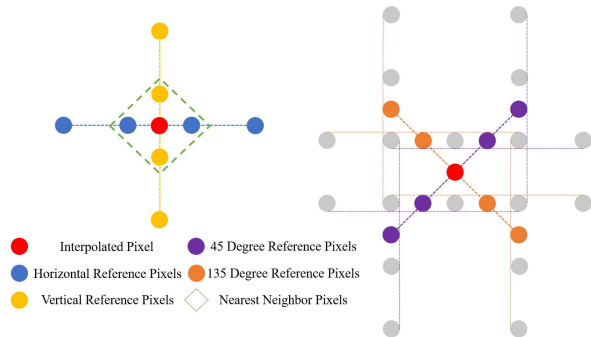


Figure 6 Cross-Shaped Interpolation

3.3 Adaptive Edge-Directed Interpolation

The proposed image interpolation scheme is composed of a combination of existing image interpolation schemes. We use a bilinear, bicubic interpolation method with reference to LR pixels. If there is no reference pixel, interpolation is performed after generating the reference pixel using the cubic spline interpolation.

If the pixel to be interpolated is a flat pixel, a bilinear interpolation method using four surrounding pixels is performed.

Test Sequences 512 x 512			
	mandril	barbara	lion
wheel	lena	butterfly	cameraman
house	jetplane	peppers	boat

Figure 7 Test Sequences (512x512)

When it is determined to be an edge pixel, the interpolation method is determined considering the flat/edge characteristics and the directionality of the four surrounding pixels. We confirm that the directionality of the four surrounding pixels has a dominant direction, and apply the bicubic

interpolation method in that direction if there is dominant directionality. If there is no dominant directionality, the direction of interpolation is determined by the variance comparison of the reference pixels used in each of the four directions and the bicubic interpolation method is applied.

In case of the texture pixel, the bilinear and bicubic interpolation methods are selectively applied through the variance comparison of the reference pixels used for each of the four directional interpolation and the surrounding four pixels.

4 Experimental Process and Results

4.1 Experimental Implementation

As shown in Fig.7, 11 experimental images of 512x512 size were used and the input image was downsampled to 256x256 size. The original image is used as a reference image for objective image quality evaluation in the derivation of experimental results. Bilinear, bicubic interpolation and NEDI were selected as comparison algorithms. PSNR (Peak Signal-to-Noise Ratio), EPSNR (Edge PSNR), MSSIM (Mean Structural SIMilarity) and execution time were selected as performance comparison measures.

The PSNR can be calculated using the MSE (Mean Square Error). However, it does not accurately reflect the cognitive ability of the HVS (Human Visual System). Therefore, the EPSNR for evaluating the image quality of the edge region and the MSSIM for evaluating the structural similarity are additionally used. The PSNR is calculated using Eq. (3), and the EPSNR and MSSIM calculation methods are presented as references [9,10].

$$MSE = \frac{1}{w \cdot h} \sum_{i=1}^w \sum_{j=1}^h [I_{ori}(i, j) - I_{rec}(i, j)]^2$$

$$PSNR = 10 \cdot \log_{10} \left(\frac{MAX_I^2}{MSE} \right) \quad (3)$$

w and h represent the number of rows and columns of the image, and i and j represent pixel positions. I_{ori} and I_{rec} are the original image and the reconstructed image, respectively, and MAX_I indicates the maximum luminance value of the image pixel.

4.2 Experimental Results

From the objective test results shown in Table 3 to Table 6, it can be seen that the performance of the proposed algorithm is excellent. Through the results

of PSNR, EPSNR and MSSIM used in objective image quality evaluation, it can be confirmed that the proposed algorithm is more similar to the original image than the comparison algorithm. In addition, the proposed algorithm requires much more execution time than the most basic method, the bilinear and bicubic interpolation method, but it takes less time than the typical edge-directed interpolation algorithm NEDI.

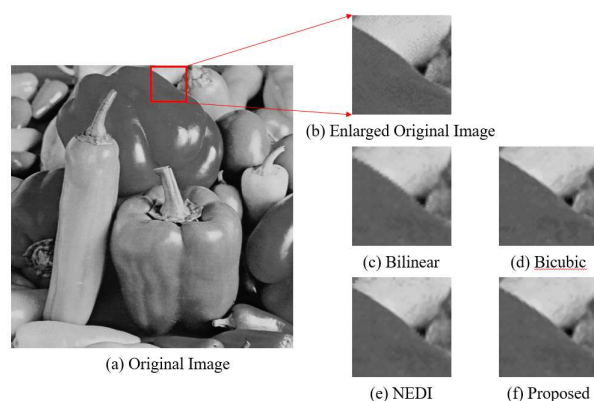


Figure 8 Subjective Quality Comparison of Interpolated Image 'peppers'

Fig.8 shows the comparison and analysis of the subjective image quality of the interpolated image. Assuming that the proposed algorithm selects the interpolation method of bilinear and bicubic interpolation, the proposed algorithm has the best performance. Comparing the images (c), (d) and (f), it can be seen that (c) shows stair-case artifact in the edge region and (d) shows that the detail of the flat region disappears. We can confirm that certain artifacts have disappeared in image (f) where interpolation is performed through proper combination of the two methods.

The above experimental results are the result of selecting the interpolation method used in the proposed algorithm as a bilinear and bicubic interpolation method. It can be expected that the edge-directed interpolation will be much better when it is replaced.

5 Conclusion

In this paper, we propose an algorithm to perform edge-directed pixel interpolation adaptively according to pixel characteristics and distribution through edge map analysis. Compared with existing algorithms, it improves objective and subjective image quality and has shorter execution time than conventional edge-directed interpolation algorithm.

Sequences	Bilinear	Bicubic	NEDI	Proposed
mandril	29.656	27.468	28.669	29.622
barbara	25.140	23.295	20.073	24.640
lion	29.637	28.693	29.484	29.720
wheel	26.472	26.415	26.422	26.845
lena	33.015	33.153	33.817	33.832
butterfly	29.244	30.512	30.572	30.384
cameraman	34.767	35.461	34.411	37.079
house	42.877	45.669	42.316	46.563
jetplane	32.484	32.567	32.519	33.478
peppers	32.201	32.057	32.151	32.597
boat	28.918	28.825	29.167	29.201
Average	31.310	31.283	30.873	32.178

Table 3 PSNR Results (dB)

Sequences	Bilinear	Bicubic	NEDI	Proposed
mandril	26.838	23.693	24.513	26.416
barbara	20.799	19.292	14.370	21.200
lion	24.496	23.453	24.116	24.552
wheel	24.070	24.945	24.572	24.981
lena	24.881	26.276	26.631	26.379
butterfly	19.589	21.216	21.001	20.811
cameraman	26.486	27.486	25.602	29.524
house	32.076	35.906	34.130	32.335
jetplane	24.328	24.520	24.417	25.295
peppers	24.659	26.189	24.746	25.731
boat	21.553	21.761	22.087	21.793
Average	24.525	24.976	24.199	25.365

Table 4 EPSNR Results (dB)

Sequences	Bilinear	Bicubic	NEDI	Proposed
mandril	0.918	0.869	0.908	0.918
barbara	0.813	0.777	0.772	0.808
lion	0.860	0.836	0.863	0.863
wheel	0.798	0.792	0.802	0.806
lena	0.911	0.902	0.916	0.916
butterfly	0.943	0.947	0.952	0.951
cameraman	0.964	0.963	0.963	0.970
house	0.988	0.989	0.988	0.991
jetplane	0.944	0.937	0.944	0.949
peppers	0.851	0.830	0.851	0.853
boat	0.839	0.828	0.843	0.845
Average	0.893	0.879	0.891	0.897

Table 5 MSSIM Results

Sequences	Bilinear	Bicubic	NEDI	Proposed
mandril	0.028	0.035	6.881	3.817
barbara	0.024	0.042	6.342	2.760
lion	0.023	0.032	6.255	3.213
wheel	0.028	0.036	7.288	2.734
lena	0.029	0.036	5.464	2.593
butterfly	0.023	0.036	5.613	2.497
cameraman	0.027	0.038	5.825	2.225
house	0.025	0.042	5.171	2.058
jetplane	0.028	0.043	6.011	3.011
peppers	0.022	0.037	5.121	2.219
boat	0.029	0.032	5.603	2.640
Average	0.026	0.037	5.961	2.706

Table 6 Execution Time Results (s)

Acknowledgements: This research was supported by Basic Science Research Program through the National Research Foundation of Korea(NRF) funded by the Ministry of Science, ICT and future Planning(NRF-2015R1A2A2A01006004)

References:

- [1] R. C. Gonzalez and R. E. Woods, *Digital Image Processing*, 3rd Edition, Prentice Hall, New Jersey, 2010.
- [2] H. S. Hou and H. C. Andrews, Cubic Splines for Image Interpolation and Digital Filtering, *IEEE Trans. Acoust., Speech, Signal Proces.*, Vol.26, No.6, Dec. 1978, pp. 508-517.
- [3] R. G. Keys, Cubic Convolution Interpolation for Digital Image Processing, *IEEE Trans. Acoust., Speech, Signal Proces.*, Vol.29, No.6, Dec. 1981, pp. 1153-1160.
- [4] S. G. Chang, Z. Cvetkovic and M. Vetterli, Locally Adaptive Wavelet-Based Image Interpolation, *IEEE Trans. Image Proces.*, Vol.15, No.6, June 2006, pp. 1471-1485.
- [5] H. Demirel and G. Anbarjafari, Discrete Wavelet Transform-Based Satellite Image Resolution Enhancement, *IEEE Trans. Geosci. Remote Sens.*, Vol.49, No.6, June 2011, pp. 1997-2004.
- [6] X. Li and M. T. Orchard, New Edge-Directed Interpolation, *IEEE Trans. Image Proces.*, Vol.10, No.10, Oct. 2001, pp. 1521-1527.
- [7] S. S. Rifman, Digital Rectification of ERTS Multispectral Imagery, *Proc. Symp. Significant Results Obtained from ERTS-1(NASA SP-327)*, sec.B, 1973, pp. 1131-1142.
- [8] R. Bernstein, Digital Image Processing of Earth Observation Sensor Data, *IBM Journal of Research and Development*, Vol.20, Jan. 1976, pp. 40-57.
- [9] C. Lee, S. Cho, J. Choe, T. Jeong, W. Ahn, and E. Lee, Objective Video Quality Assessment, *Optical Engineering*, Vol.45, No.1, Jan. 2006, pp. 1-11.
- [10] Z. Wang, A. C. Bovik, H. R. Sheikh, and E. P. Simoncelli, Image Quality Assessment: From Error Visibility to Structural Similarity, *IEEE Trans. Image Proces.*, Vol.13, No.4, April 2004, pp. 600-612.